TU Delft

Delft University of Technology

Document Version
Final published version

Licence
Dutch Copyright Act (Article 25fa)

Citation (APA)
Tocci, F., Chauvat, G., Rius-Vidales, A. F., Kotsonis, M., Hein, S., & Hanifi, A. (2026). Interaction of Crossflow Modes with Forward-Facing Steps: Insights Gained from DNS. In K. Kato, A. Inasawa, & M. Matsubara (Eds.), *Proceedings of the 10th IUTAM Symposium on Laminar-Turbulent Transition* (pp. 63-69). Springer. https://doi.org/10.1007/978-981-96-9829-5_9

Important note
To cite this publication, please use the final published version (if applicable).
Please check the document version above.

Copyright
In case the licence states “Dutch Copyright Act (Article 25fa)”, this publication was made available Green Open Access via the TU Delft Institutional Repository pursuant to Dutch Copyright Act (Article 25fa, the Taverne amendment). This provision does not affect copyright ownership.
Unless copyright is transferred by contract or statute, it remains with the copyright holder.

Sharing and reuse
Other than for strictly personal use, it is not permitted to download, forward or distribute the text or part of it, without the consent of the author(s) and/or copyright holder(s), unless the work is under an open content license such as Creative Commons.

Takedown policy
Please contact us and provide details if you believe this document breaches copyrights.
We will remove access to the work immediately and investigate your claim.

This work is downloaded from Delft University of Technology.

Chapter 9
Interaction of Crossflow Modes with Forward-Facing Steps: Insights Gained from DNS



F. Tocci, G. Chauvat, A. F. Rius-Vidales, M. Kotsonis, S. Hein, and A. Hanifi

Abstract Surface roughness, such as forward-facing steps (FFS), significantly impacts the laminar-turbulent transition in swept-wing boundary layers. This study employs direct numerical simulations (DNS) to investigate the non-monotonic relationship between FFS height and transition location, complementing recent experimental findings. Two step heights and a baseline clean surface are analyzed under experimentally representative conditions. The simulations confirm a delay in transition for the shallow FFS and premature transition for the higher FFS, reproducing experimental trends while revealing some discrepancies in the abruptness of transition advancement for the larger step. DNS results provide detailed insights into the interaction of crossflow modes with the FFS, particularly near the step, highlighting the spanwise modulation and the formation of reverse flow regions.

Keywords Direct numerical simulation · Crossflow instability · Forward-facing steps

9.1 Introduction

In recent studies, both experiments (e.g. [1, 2]) and numerical simulations (e.g. [3]) have explored how surface roughness, specifically forward-facing steps (FFS), affects laminar-turbulent transition in swept-wing boundary layers with crossflow instabilities (CFI). Casacuberta et al. [3] focused on steady direct numerical simu-

F. Tocci (✉) · S. Hein
Institute of Aerodynamics and Flow Technology, German Aerospace Center (DLR), Göttingen, Germany
e-mail: francesco.tocci@dlr.de

G. Chauvat · A. Hanifi
FLOW, Department of Engineering Mechanics, KTH Royal Institute of Technology, Stockholm, Sweden

A. F. Rius-Vidales · M. Kotsonis
Department of Flow Physics and Technology, Delft University of Technology, Delft, The Netherlands

© The Author(s), under exclusive license to Springer Nature Singapore Pte Ltd. 2026

K. Kato et al. (eds.), *Proceedings of the 10th IUTAM Symposium on Laminar-Turbulent Transition*, IUTAM Bookseries 44, https://doi.org/10.1007/978-981-96-9829-5_9

lation (DNS), in which no transition occurred, to investigate stationary mechanisms near the FFS on a flat-plate configuration with an imposed pressure gradient, where the stationary crossflow (CF) amplitude remained in the linear regime up to the FFS. The experimental observations of Rius-Vidales and Kotsonis [2] revealed a non-monotonic relationship between step height and the location of transition. Notably, an unprecedented delay in transition—compared to scenarios without FFS—occurs when stationary CF vortices interact with a shallow FFS, while interaction with a higher FFS leads to an upstream advancement of the transition front. Motivated by these experimental findings, the present work aims to replicate the setup and conditions described in [2] via DNS. In addition to reproducing the transition trends, this study examines the interaction of CF vortices with the FFS, highlighting the associated formation of reverse flow regions.

9.2 Flow Conditions and Methodology

The experimental setup described in [2] features the M3J swept-wing model with a sweep angle of $\Lambda = 45°$ and a chord length normal to the leading edge of $c_x = 0.9\,\mathrm{m}$. The model is mounted vertically in the Low Turbulence Tunnel at the Delft University of Technology at an angle of attack $\mathrm{AoA} = -3°$. Discrete roughness elements (DREs) near the leading edge are used to trigger a stationary primary CF mode with a spanwise wavelength $\lambda_0 = 7.5\,\mathrm{mm}$.

The numerical simulations employ a Cartesian coordinate system (x, y, z), where x is oriented perpendicular to the leading edge of the wing (chordwise), z is parallel to the leading edge (spanwise), and y is normal to both x and z (Fig. 9.1). The velocity components in this system are denoted as U, V, W along the x, y, z directions, respectively. For result presentation, a curvilinear reference system (x_τ, y_η, z) is used, where x_τ is the chordwise direction tangent to the wing surface and y_η is normal to the wing surface. In this system, the velocity components are denoted as u_τ, v_η, w. The freestream velocity for the simulations is set to $U_\infty = 27.542\,\mathrm{m\,s^{-1}}$, corresponding to a chord Reynolds number given by $Re_{c_x} = U_\infty c_x/\nu = 1.68 \times 10^6$. Three-dimensional (3D) DNS are conducted for the clean case (denoted as s0) and FFSs of two heights, s1 ($h = 368\,\mu\mathrm{m}$, $Re_{hh} = u_{\tau_h} h/\nu = 205$, where u_{τ_h} represents the u_τ at the FFS height and FFS chordwise location for the clean basic flow) and s2 ($h = 474\,\mu\mathrm{m}$, $Re_{hh} = 322$). The computational domain for the 3D DNS spans a single spanwise wavelength λ_0, with periodic boundary conditions applied along the z-direction. The 3D DNS, constrained by the relatively small domain C in Fig. 9.1, relies on precise boundary conditions derived from a preliminary spanwise-invariant (2.5D) RANS simulation covering the entire airfoil shape and wind tunnel walls. Subsequently, a 2.5D DNS is conducted for the domain B in Fig. 9.1. The effect of DREs used to condition the instability modes in the experiments is accurately reproduced via perturbations computed through nonlinear parabolised stability equations, which are applied as inflow conditions for the 3D DNS. Unsteady noise is also added as a random forcing in the boundary layer close to the inflow such that the laminar-

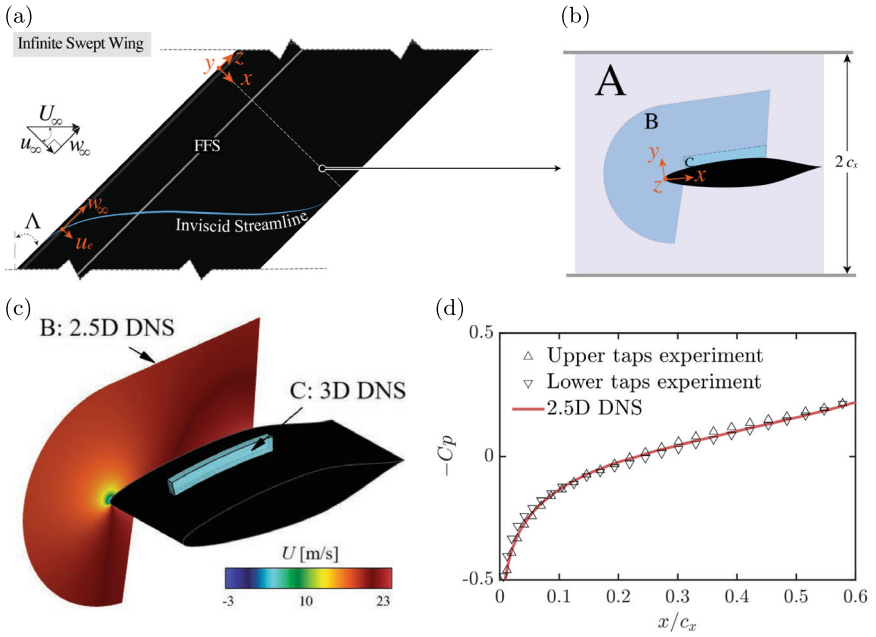


Fig. 9.1 (**a**) Schematic of the M3J infinite swept-wing model. (**b**) Cross-sectional view of a plane normal to the leading edge, showing the wind tunnel walls and computational domains: A for 2.5D RANS, B for 2.5D DNS, and C for 3D DNS. (**c**) Contours of the velocity component U for the clean case from the 2.5D DNS (domain B), with domain C for the 3D DNS highlighted in cyan. (**d**) Comparison of the pressure coefficient C_p between the 2.5D DNS results and experimental data for the clean case

turbulent transition in the simulations approximates that in the experiments for the clean case s0. Further details can be found in [4]. DNS are performed using the spectral element method (SEM) code Nek5000 [5], with a polynomial order $P = 9$.

9.3 Transition Behaviour and CFI Interaction with FFS

Figure 9.2 compares the skin-friction coefficients for s0, s1, and s2, presenting DNS results averaged in time and along the spanwise direction, alongside confidence intervals derived from experimental measurements. The DNS results confirm a delay in transition for FFS s1 and a premature transition for FFS s2, reflecting the non-monotonic relationship between step height and transition location observed in experiments [2]. While the delay associated with s1 shows a relatively good agreement with experimental data, the transition advancement for s2 is noticeably more pronounced in the DNS. This suggests that s2 exhibits supercritical behavior in the simulations, differing from its classification as critical in the experiments. For a detailed analysis

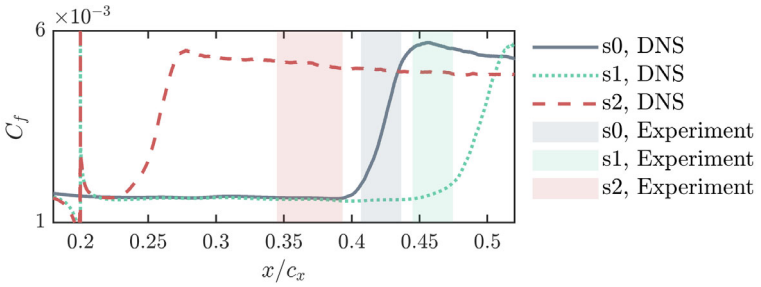


Fig. 9.2 Comparison of skin-friction coefficients for s0, s1, and s2: DNS results (temporally and spanwise averaged) alongside confidence intervals from experimental measurements of the transition location obtained using infrared thermography

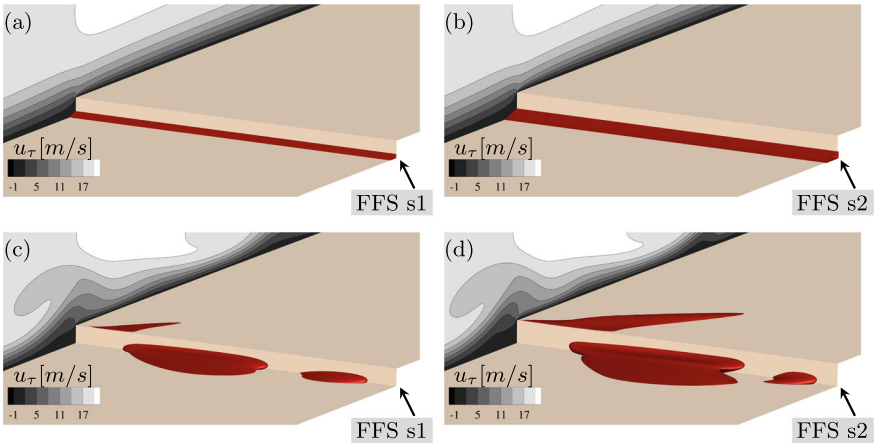


Fig. 9.3 Visualisation of the 2.5D basic flow (**a**, **b**) and the time-averaged 3D DNS (**c**, **d**). (**a**, **c**) correspond to s1 and (**b**, **d**) correspond to s2. The 2.5D basic flows, spanwise-uniform by definition, are extruded for λ_0 to enable comparison. Reverse flow regions are indicated by red isosurfaces of $u_\tau = 0$, with grey scale contours of the time-averaged u_τ shown for the plane $x_\tau y_\eta$ at $z = -\lambda_z/2$

of the mechanisms underlying the transition behaviour for s0, s1 and s2 the reader is referred to [4].

Figure 9.3 compares the reverse flow regions ($u_\tau = 0$) for s1 and s2 in the 2.5D basic flows (Fig. 9.3a, b) and the 3D time-averaged flows (Fig. 9.3c, d) resulting from the interaction of stationary CF vortices with the FFS. In the basic flows, both s1 and s2 exhibit a single reverse flow region upstream of the step, with its size increasing with the step height, resulting in a larger region for s2 compared to s1. Due to the stationary CF vortices in the 3D flows, the reverse flow regions are strongly modulated in the spanwise direction, resulting in isolated zones of reversed flow, both upstream and downstream of the FFS. An analysis of several instantaneous flow fields (not shown) indicates the nearly stationary nature of the spanwise-modulated

reverse flow regions. The spanwise modulation of the flow is particularly evident in the 3D fields for s1 and s2, as shown in Fig. 9.4, where the clean case s0 serves as a baseline for comparison. As noted in [1], the modulation of the reverse flow regions is strongly influenced by the amplitude of the stationary CF at the onset. In the present study, the primary CFI reaches the FFS location with a relatively high amplitude, with the maximum CFI spanwise velocity reaching approximately 13% of the local freestream spanwise velocity, leading to a strong spanwise deformation of the shear layer. Compared to the clean configuration, the trajectory of the primary CF vortex (identified using the Q-criterion) is significantly altered in the presence of a FFS, deviating from its original path and interacting with the reverse flow region. At the location of interaction between the CF vortex and the FFS, the reverse flow region observed in the basic flow disappears. However, downstream of the FFS edge, a relatively thin yet elongated reverse flow region forms near the wall. Upstream of the step, the spanwise-modulated reverse flow region exhibits a larger volume compared to its uniform counterpart in the basic flow (Fig. 9.3). Additionally, secondary spanwise-oriented vortical structures emerge within the largest reverse flow region upstream of the step and near the wall downstream of the FFS. For the higher step s2, a secondary vortical structure develops further downstream, closely aligned with the trajectory of the primary CF vortex and located near the wall. The amplitude of the stationary CF vortex in a localized region downstream of the FFS is reduced compared to the clean case, as detailed in [4]. While the higher FFS s2 induces greater overall distortion than s1, the qualitative similarities in the observed flow field distortions suggest that time-averaged flow characteristics alone are inadequate to fully explain the transition trends. This emphasizes the need to consider unsteady mechanisms and secondary instability interactions for a comprehensive understanding of the observed transition behavior.

9.4 Conclusion

This study successfully reproduces the non-monotonic relationship between FFS height and transition location observed in experiments, confirming a delay for the shallow step and premature transition for the higher step. DNS reveal spanwise-modulated reverse flow regions extending both upstream and downstream of the FFS, resulting from the interaction of stationary CF vortices with the FFS. Despite the greater distortion induced by the higher step, the qualitative similarity in time-averaged flow field characteristics across step heights points to the importance of investigating secondary instabilities and unsteady mechanisms for a more comprehensive interpretation of the transition process.

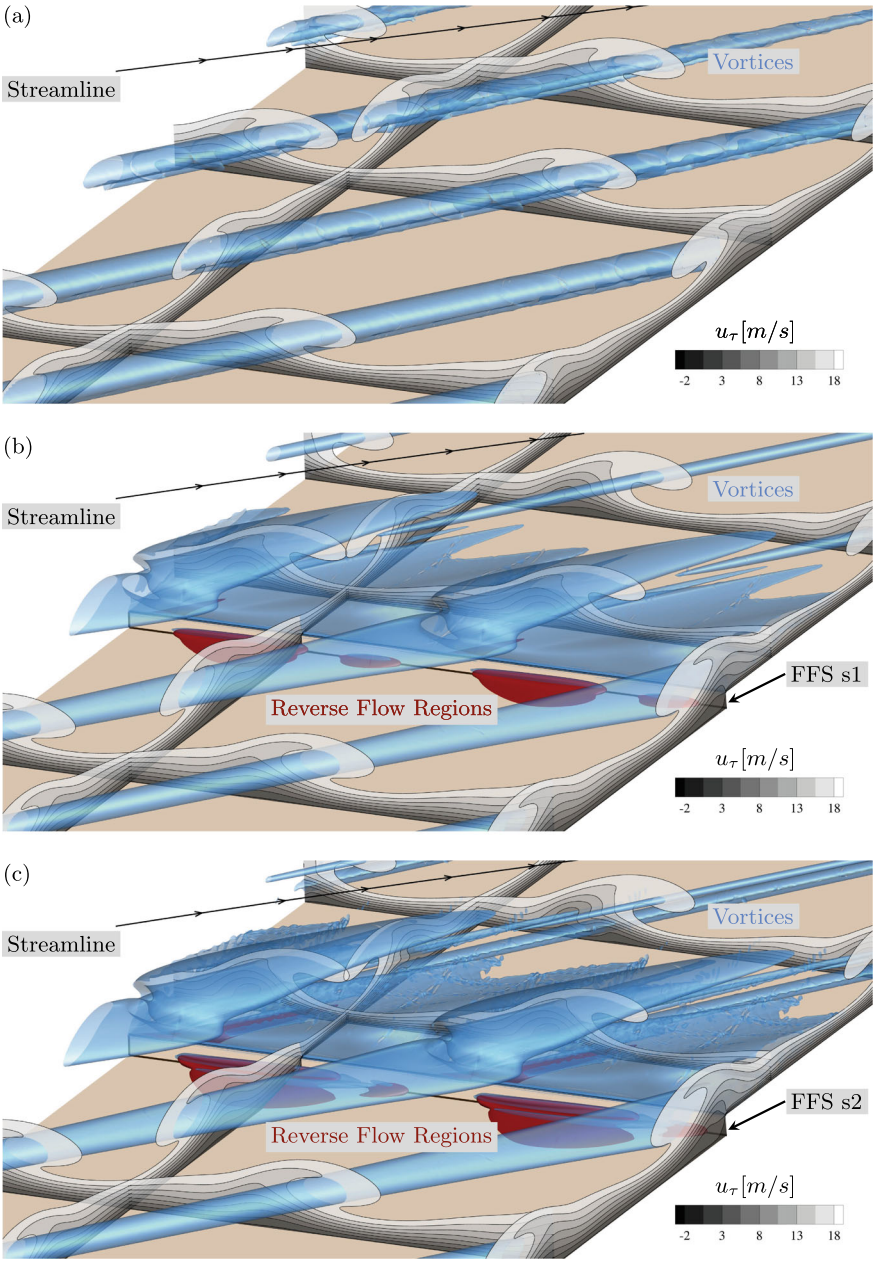


Fig. 9.4 Visualisation of the time-averaged flow field development for s0 (**a**), s1 (**b**), and s2 (**c**). Reverse flow regions are indicated by the red isosurface of $u_\tau = 0$, while vortical structures are represented by a light blue isosurface of the Q-criterion. Grey scale contours of the time-averaged u_τ are shown for multiple slices in the $x_\tau y_\eta$ and $z y_\eta$ planes. The domain is duplicated in the spanwise direction for visualization purposes

Acknowledgements F. Tocci and S. Hein gratefully acknowledge the scientific support and HPC resources provided by the German Aerospace Center (DLR). The HPC system CARO is partially funded by the Ministry of Science and Culture of Lower Saxony and the Federal Ministry for Economic Affairs and Climate Action. F. Tocci and G. Chauvat acknowledge funding from the European Union's Horizon 2020 research and innovation programme through the Marie Skłodowska-Curie grant agreement No. 675008. G. Chauvat has also been funded through the European Research Council under grant agreement 694452-TRANSEP-ERC-2015-AdG.

References

1. Eppink, J.L.: Mechanisms of stationary cross-flow instability growth and breakdown induced by forward-facing steps. J. Fluid Mech. **897**, A15 (2020). https://doi.org/10.1017/jfm.2020.367
2. Rius-Vidales, A.F., Kotsonis, M.: Impact of a forward-facing step on the development of cross-flow instability. J. Fluid Mech. **924**, A34 (2021). https://doi.org/10.1017/jfm.2021.689
3. Casacuberta, J., Hickel, S., Westerbeek, S., Kotsonis, M.: Direct numerical simulation of interaction between a stationary crossflow instability and forward-facing steps. J. Fluid Mech. **943**, A46 (2022). https://doi.org/10.1017/jfm.2022.456
4. Tocci, F., Chauvat, G., Rius-Vidales, A.F., Kotsonis, M., Hein, S., Hanifi, A.: Crossflow instability interaction with forward-facing steps: direct numerical simulation of transition. To be submitted (2025)
5. Fischer, P.F., Lottes, J.W., Kerkemeier, S.G.: Nek5000 Web Page (2008). http://nek5000.mcs.anl.gov